



HHS Public Access

Author manuscript

Mucosal Immunol. Author manuscript; available in PMC 2016 May 18.

Published in final edited form as:

Mucosal Immunol. 2016 May ; 9(3): 610–620. doi:10.1038/mi.2015.85.

Bone marrow transplantation alters lung antigen presenting cells to promote T_H17 response and the development of pneumonitis and fibrosis following gammaherpesvirus infection

Xiaofeng Zhou¹, Hillary Loomis-King¹, Stephen J. Gurczynski¹, Carol A. Wilke¹, Kristine E. Konopka², Catherine Ptaschinski², Stephanie M Coomes³, Yoichiro Iwakura⁴, Linda F. van Dyk⁵, Nicholas W. Lukacs², and Bethany B. Moore^{1,6}

¹Department of Internal Medicine, Pulmonary and Critical Care Medicine Division, University of Michigan, Ann Arbor, MI

²Department of Pathology, University of Michigan, Ann Arbor, MI

³Graduate Program in Immunology, University of Michigan, Ann Arbor, MI

⁴Research Institute for Biomedical Sciences, Tokyo University of Science, Noda, Chiba, Japan

⁵Department of Immunology and Microbiology, University of Colorado School of Medicine, Aurora, CO

⁶Department of Microbiology and Immunology, University of Michigan, Ann Arbor, MI

Abstract

Hematopoietic stem cell transplantation (HSCT) efficacy is limited by numerous pulmonary complications. We developed a model of syngeneic bone marrow transplant (BMT) followed by infection with murine gamma herpesvirus (γ HV-68) that results in pneumonitis and fibrosis and mimics human “non-infectious” HSCT complications. BMT mice experience increased early lytic replication, but establish viral latency by 21 days post infection (dpi). CD4 T cells in BMT mice are skewed towards IL-17A rather than IFN- γ production. Transplantation of bone marrow from *Il-17a*^{-/-} donors or treatment with anti-IL-17A neutralization antibodies at late stages attenuates pneumonitis and fibrosis in infected BMT mice, suggesting that hematopoietic-derived IL-17A is essential for development of pathology. IL-17A directly influences activation and extracellular matrix production by lung mesenchymal cells. Lung CD11c+ cells of BMT mice secrete more TGF- β 1, and pro-T_H17 mRNAs for IL-23 and IL-6, and less T_H1-promoting cytokine mRNA for IFN- γ but slightly more IL-12 mRNA in response to viral infection. Adoptive transfer of non-BMT lung CD11c-enriched cells restores robust T_H1 response and suppresses aberrant T_H17 response in BMT mice to improve lung pathology. Our data suggest “non-infectious” HSCT lung complications may reflect preceding viral infections and demonstrate that IL-17A neutralization may offer therapeutic advantage even after disease onset.

Users may view, print, copy, and download text and data-mine the content in such documents, for the purposes of academic research, subject always to the full Conditions of use:http://www.nature.com/authors/editorial_policies/license.html#terms

Corresponding author: Bethany Moore, PhD, 4053 BSRB, 109 Zina Pitcher Pl, Ann Arbor, MI 48109-2200, ; Email: Bmoore@umich.edu, (734)647-8378 phone, (734)615-2331 fax

There are no potential conflicts of interest to disclose regarding this work.

Introduction

Hematopoietic stem cell transplantation (HSCT) is a potentially curative therapy for inherited genetic disorders, autoimmune diseases and malignancies. However, the usefulness of this therapy is limited by the development of lung complications which occur in 30–60% of HSCT patients, and are associated with significant morbidity and mortality^{1, 2}. During HSCT, a recipient may receive hematopoietic stem cells from a histocompatibility antigen-matched donor or from him/herself (allogeneic or autologous HSCT). Recent multi-country surveys found that ~42% of the HSCT procedures are allogeneic while ~58% are autologous HSCT³.

Pulmonary complications (infectious and noninfectious) can occur in both allogeneic and autologous HSCT, but tend to be more frequent in allogeneic HSCT recipients¹. Infectious pneumonia can be caused by fungi, bacteria or viruses and can occur even after full hematopoietic reconstitution⁴. The occurrence of noninfectious pulmonary complications follows a characteristic time pattern^{1, 2}. Engraftment syndrome, diffuse alveolar hemorrhage, and periengraftment respiratory distress syndrome usually occur during the first 30 days following transplant. Bronchiolitis obliterans syndrome (BOS) and cryptogenic organizing pneumonia (COP) usually occur late post-transplantation⁵. Nonspecific interstitial fibrosis can also occur during the late post-transplant period^{2, 6}. Idiopathic pneumonia syndrome (IPS) can occur at any time following transplant⁷. Late stage complications that manifest following hematopoietic reconstitution result in severe and often fatal lung dysfunction². Unfortunately, the etiology and pathogenesis of IPS, BOS, COP and nonspecific interstitial fibrosis are all poorly understood.

Noninfectious late complications are often diagnosed by the absence of apparent infection at the time of symptom onset, although recent evidence suggests some cases of IPS may have occult infections⁸. Additionally, these complications may represent pathologic sequelae that are initially triggered by a preceding viral infection even if the lytic infection is cleared by the time of diagnosis^{9, 10}. For example, a prospective study of pediatric allogeneic HSCT recipients found that early respiratory virus infection post-HSCT was correlated significantly with the later development of IPS and BOS¹⁰. Many of the noninfectious complications including IPS, BOS and COP manifest with lung fibrosis, a scarring process that excessively deposits extracellular matrix, especially collagen, causing stiffness and reducing oxygen diffusion capacity at the later stages². In general, lung fibrosis is believed to represent a dysregulated wound healing response to lung injury. Viral infections have been suggested to mediate lung injury that leads to some forms of pulmonary fibrosis¹¹. For example, Epstein-Barr virus (EBV), cytomegalovirus (CMV), human herpes viruses (HHV)-7 and Kaposi's sarcoma associated herpesvirus (KSHV) are often found in lung tissue of human familial and idiopathic pulmonary fibrosis (IPF) patients (reviewed in¹¹). In addition, infection with murine gamma herpesvirus-68 (γ HV-68) can lead to fibrosis in aged or Th2-biased mice¹¹. To determine whether gammaherpesvirus can contribute to the development of lung dysfunction in the context of HSCT, we previously established a murine model of infection following bone marrow transplantation (BMT). In this model, fully hematopoietic reconstituted syngeneic or allogeneic BMT mice are infected with murine gamma

herpesvirus-68 (γ HV-68), which is genetically related to human EBV and KSHV^{12, 13}. Allogeneic BMT mice die starting by day 10 when infected with γ HV-68; however, syngeneic BMT (hereafter referred to as just BMT) mice infected with γ HV-68 develop interstitial pneumonitis and fibrosis that persists after lytic viral infection has been cleared, at a time point when the virus has established latency¹² (Supplementary Figure 1 online). The inflammatory and fibrotic pathology that develops in these mice shares features of IPS, BOS, COP and nonspecific fibrosis that also complicate human HSCT.

In our γ HV-68-infected BMT mouse pneumonitis and fibrosis model, we previously demonstrated an increase in the percentage of CD4 T cells that produce IL-17A and a concomitant reduction in CD4 cells producing IFN- γ ¹². In this study, we aimed to investigate the mechanisms that underlie the development of pneumonitis and fibrosis in fully reconstituted BMT mice after γ HV-68 infection. Here we report that transplantation of bone marrow cells from *Il-17a*^{-/-} mice or neutralization of IL-17A greatly attenuated pneumonitis and fibrosis induced by γ HV-68 infection in BMT mice. Lung antigen presenting cells (APCs) are critical in priming T helper cells to differentiate into T_H17 cells by producing increased amounts of TGF- β 1, IL-6 and IL-23 post-HSCT in response to γ HV-68. IL-17A has direct effects on fibroblasts by stimulating their proliferation and extracellular matrix secretion. Thus, this model allows us to understand how innate and adaptive immune responses to a respiratory virus are altered in the setting of HSCT and provide insight into potential etiologies of “non-infectious” pulmonary complications following HSCT therapy.

Results

BMT mice are impaired in restricting γ HV-68 lytic replication and develop pulmonary fibrosis by 21 dpi

To understand viral host defense and pulmonary complications post-HSCT, we have developed a BMT mouse model^{12, 13}. Recipient C57BL/6 mice are lethally irradiated followed by syngeneic BMT. Hematopoietic reconstitution of the periphery and lung is complete by 5 weeks post-BMT when assessed by CD45.1 and CD45.2 haplotypes¹⁴; thus viral infection with γ HV-68 occurs at a time of full hematopoietic reconstitution. We infected mice with recombinant γ HV-68 harboring an EYFP-tagged histone H2B to allow quantitation of the numbers of infected cells¹⁵. In BMT mice, viral infected cells were detectable starting at three days post infection (dpi), with most infected cells appearing in clusters, especially near airways, indicating active replication and transmission of virus (Figure 1a). In non-BMT mice, infected cells were rarely detectable until 7 dpi, with scattered infected cells indicating limited cell to cell infection (Figure 1a). There were significantly more viral infected cells in BMT lungs than in non-BMT lungs at both 3 and 7 dpi (Figure 1b). At 21 dpi, both BMT and non-BMT mice had few EYFP^{H2B} positive cells; confirming both BMT and non-BMT mice had established a latent infection by 21 dpi¹².

To quantify differences in early viral lytic replication between BMT and non-BMT mice, mRNA was isolated from both groups of mice at designated dpi, and real-time RT-PCR was performed to measure lytic viral gene expression. An ~140-fold increase in the expression of viral DNA polymerase (Figure 1c) and envelope glycoprotein gene *gB* (data not shown) was

detected at 3 dpi in BMT mice but this difference was reduced to about 3-fold at 7 dpi (Figure 1c), consistent with our earlier report¹³. BMT mice experience increased lung injury post-infection in response to the viral replication within the first 7 dpi as noted by an increase in the protein concentration in the bronchoalveolar lavage (BAL) fluid (Supplementary Figure 2a online). The virus establishes latency by 14 dpi¹⁶ and maintains latency through 21 dpi in both BMT and non-BMT mice^{12, 16}, with little lytic gene expression detectable at this time point (Figure 1c).

Reactivation of γ HV-68 is not required to develop pulmonary fibrosis in BMT mice

Pulmonary fibrosis can be induced by γ HV-68 in T_H2 -biased *IFN- γ R*^{-/-} mice through reactivation of latent virus¹⁷. To determine whether reactivation of latent γ HV-68 in BMT lungs is important for the development of pulmonary fibrosis, we infected BMT mice with either a γ HV-68 mutant containing a stop codon within ORF 72 (v-cyclin.stop)¹⁸ or the wild type virus. The v-cyclin.stop virus undergoes normal lytic replication during acute infection but has greater than a 100-fold reduction in the ability to reactivate from latency¹⁸. At 21 dpi, v-cyclin.stop viruses caused pulmonary fibrosis that was just as severe as the wild type virus (Figure 2a–b). Thus, γ HV-68 viral reactivation is not required for the development of pulmonary fibrosis in BMT mice. To further define the window during which viral lytic replication is critical for later fibrotic pathology, we treated γ HV-68-infected BMT mice with cidofovir, a nucleoside analogue that competitively inhibits the incorporation of deoxycytidine triphosphate into viral DNA by viral DNA polymerase¹⁹, starting at various time points. Administration of cidofovir before 4 dpi significantly protected BMT mice from development of pneumonitis and pulmonary fibrosis at 21 dpi, while administration of cidofovir after 4 dpi, had no significant effect as noted in the pathologic scoring of tissues (Figure 2c).

Infected BMT mice are characterized by increased T_H17 and decreased T_H1 differentiation

We next compared the kinetics of helper T cell differentiation in infected non-BMT and BMT mice. In BMT mice, the percent of T_H1 cells (expressing IFN- γ) was significantly decreased at 7 and 14 dpi, while the percent of T_H17 cells (expressing IL-17A) was continuously increased at 7, 14 and 21 dpi (Figure 3a–b). There was no significant difference among non-BMT and BMT mice in T_H2 differentiation as determined by percent of IL-4 expressing cells (Figure 3c). Given the accumulation of T_H17 cells over time in this model, we next addressed the impact of IL-17A on the disease pathogenesis.

Bone marrow-derived IL-17A producing cells are required for development of pneumonitis and fibrosis in γ HV-68-infected BMT mice

To determine whether the increase in T_H17 cells in BMT mice is responsible for the development of lung pathology post-infection, we transplanted bone marrow of *Il-17a*^{-/-} mice on a C57BL/6 background²⁰ into C57BL/6 mice, confirmed full hematopoietic reconstitution (5 weeks) and then infected with γ HV-68. We saw striking protection from pneumonitis and fibrosis in the mice that received *Il-17a*^{-/-} bone marrow at 21 dpi (Figure 4a–b). To determine whether a somatic source of IL-17A is necessary for development of lung pathology, we transplanted marrow of wild type mice into *Il-17a*^{-/-} mice and then infected with γ HV-68. These mice were not protected from pneumonitis or fibrosis (Figure

4a–b). To determine whether IL-17A has any impact on acute viral replication in either BMT or non-BMT mice, we infected WT or *Il-17a*^{-/-} mice or BMT mice (WT into WT vs. *Il-17a*^{-/-} into WT) with γ HV-68 and measured acute lytic viral replication. Loss of IL-17A did not impact acute viral replication in either non-BMT or BMT mice (Figure 4c).

To determine whether IL-17A was promoting lung pathology via early or late actions, we administrated virally-infected BMT mice with neutralizing antibodies against IL-17A²¹ either during the priming phase (0–4 dpi) or during the effector phase (after 10 dpi) (Figure 4d). Mice receiving neutralizing antibodies against IL-17A during late time points were protected from pulmonary pathology while the ones receiving antibodies during early time points were not (Figure 4e).

IL-17A directly activates lung mesenchymal cells

Lung mesenchymal cells, including fibroblasts and fibrocytes, are major contributors to pulmonary fibrotic processes. IL-17A receptor is expressed in mesenchymal cells²². To determine whether IL-17A has direct effects on mesenchymal cells, we cultured lung mesenchymal cells isolated from C57Bl/6 mice with recombinant murine IL-17A in various concentrations. IL-17A can significantly increase mesenchymal cell proliferation as measured by uptake of ³H-thymidine (Figure 5a). Additionally, when murine mesenchymal cells were co-cultured with IL-17A, we observed that the expression of collagen type III and fibronectin first increased at 48 hours (Figure 5b) followed by increased expression of collagen type I at 72 hours (Figure 5c).

Lung APCs dictate T_H17 polarization in BMT mice

Pulmonary dendritic cells (DC), rather than alveolar macrophages, are believed to be the major APCs in the lung²³, although both express CD11c. We thus compared the characteristics of CD11c⁺ lung APCs from BMT and non-BMT mice. Previously, we found that lung-derived APCs from BMT mice expressed similar levels of MHC class II and co-stimulatory molecules, and were able to effectively stimulate mixed lymphocyte responses¹³, but their cytokine profiles were not characterized. We enriched lung APCs at 7 dpi by collecting CD11c⁺ cells from collagenase digested lungs; alveolar macrophages were minimized from this population by allowing them to adhere to culture plates. Enriched lung APCs were restimulated with γ HV-68 for 36 hours to determine their ability to produce pro-T_H17 cytokines. Indeed, APCs from infected BMT mice made significantly more TGF- β 1 and IL-6 and IL-23 mRNA (Figure 6a). Although lung APCs from infected BMT mice expressed lower mRNA levels of the pro-T_H1 cytokine IFN- γ , they expressed slightly higher levels of IL-12 mRNA (Figure 6b). Lung APCs from unchallenged mice also made more IL-6, IL-23 and IL-1 β mRNA than those from non-BMT mice when infected with equivalent doses of virus *ex vivo* for 24 hours (Figure 6c). Taken together, the differences in cytokine expression levels between the lung APCs from non-BMT and BMT mice are consistent with the skewing of T helper cell differentiation in BMT mice.

In order to determine whether T cell polarization could be directly attributed to lung APC function, we collected CD11c⁺ lung APCs from either non-BMT or BMT mice at 3 dpi, and adoptively transferred 5×10^5 CD11c⁺ enriched cells from non-BMT mice into BMT mice,

or transferred CD11c⁺ enriched cells from BMT mice into non-BMT mice (Figure 7a). The CD11c⁺ MHC class II⁺ APCs in this population were classified by flow cytometry to contain approximately 65% CD11b⁺ conventional DCs, 4% CD103⁺ conventional DCs, 18% Ly6C⁺ inflammatory DCs and 16% alveolar macrophages, while the CD11c^{dim} plasmacytoid DCs (PDCA1⁺) were not detected within this population (Figure 7b). The CD11c⁺ cells enriched from BMT lungs had a similar composition of cell types as those cells from non-BMT lungs and the total numbers of CD11c⁺ APCs that accumulated in BMT and non-BMT mice were similar (data not shown). One day post adoptive transfer, these mice were infected with γ HV-68, and lungs were harvested at 7 dpi for T_H cytokine analysis. Strikingly, BMT mice receiving APCs from non-BMT mice showed increased T_H1 and reduced T_H17 differentiation (Figure 7c). However, non-BMT mice receiving APCs from BMT mice maintained normal T helper cell differentiation. The BMT mice receiving APCs from non-BMT mice were protected from pneumonitis and fibrosis at 21 dpi (Figure 7d–e).

Discussion

BMT mice experience increased early lytic viral replication which is essential for development of lung pathology, because cidofovir treatment in the first 4 dpi can protect BMT mice from pneumonitis and fibrosis. How early lytic replication promotes eventual lung pathology is not clear. It is possible that increased viral replication causes BMT mice to experience increased lung injury post-infection. BMT mice do show evidence of lung injury in response to viral replication within the first 7 dpi as noted by increased protein concentration in the BAL, which is minimized if mice are treated simultaneously with cidofovir starting one day after infection (Supplementary Figure 2a online). This is consistent with previous observations that the absolute viral load impacts the degree of pneumonitis and fibrosis in BMT mice¹²; infection with 1×10^3 pfu γ HV-68 results in less lung pathology than 5×10^4 or 1×10^6 pfu. Interestingly, WT BMT and *Il-17a*^{-/-} into WT BMT mice experience similar levels of viral replication (Figure 4c), and similar levels of acute lung injury (Supplementary Figure 2b online) but the BMT mice with *Il-17a*^{-/-} bone marrow do not develop pneumonitis and fibrosis (Figure 4a), indicating lung injury in the absence of IL-17A is insufficient to drive the eventual lung pathology. We believe early viral replication by itself is not sufficient to drive lung pathology, but may recruit and prime lung APCs to promote the eventual T_H17 responses.

BMT mice develop an altered adaptive immune response to γ HV-68. Previous studies have suggested a T_H1 dominant response for γ HV-68 clearance in non-transplant mice²⁴. We found that T_H1 cells are diminished in the first 14 dpi in BMT mice and T_H17 cells are increased throughout 21 dpi. Our results using IL-17A-deficient mice and anti-IL-17A antibodies suggest bone marrow derived IL-17A is essential for lung pathology in infected BMT mice. Interestingly, production of IL-17A does not impact replication of γ HV-68 in either the non-BMT or the BMT setting. The fact that BMT and non-BMT mice both had few EYFP-H2b expressing cells evident at 21 dpi likely reflects clearance of the majority of the infected cells as this construct would still be predicted to be visible during latency due to the slow degradation of this fusion protein¹⁵.

Another potential explanation for the exuberant development of lung pathology in the BMT mice involves persistent reactivation of virus as seen in T_H 2-biased mice¹⁷. However, both cidofovir treatment starting at 5 dpi or use of the v-cyclin.stop virus which initially replicates at levels equivalent to the wild type virus before establishing latency¹⁸ demonstrate that persistent viral reactivation is not relevant for this pathology. The reasons for the differences in these models (BMT vs. IFN γ R^{-/-} mice) may reflect that BMT mice are deficient, but not devoid of IFN- γ signaling, that there is no alteration in T_H2 cytokine responses in BMT mice or may reflect alterations caused by conditioning. Note that while irradiation alone can cause pulmonary fibrosis after about 9 months²⁵, this is a much longer time frame than our experiments, and fibrosis and pneumonitis are not seen in our BMT mice in the absence of infection. Taken together, these results suggest the development of fibrosis relates to an altered immune response rather than ongoing viral reactivation and that IL-17A can promote the development of lung pathology without impacting the degree of acute viral replication and early lung injury.

IL-17A has been implicated in mediating other forms of lung fibrosis and HSCT complications^{26,29}. Under non-transplant conditions such as idiopathic pulmonary fibrosis, elevated levels of IL-17A are found in the bronchoalveolar lavage fluid (BALF)²⁶. Neutralization of IL-17A, IL-17A deficiency or IL-17RA deficiency in mouse models attenuates lung fibrosis induced by bleomycin^{26,27}, silica²⁷ or *Saccharopolyspora rectivirgula*³⁰. However, in our laboratory, *Il-17a*^{-/-} mice develop equivalent bleomycin-induced fibrosis as wild-type mice (data not shown) and others have reported that IL-17A does not promote silica-induced lung fibrosis³¹. Thus, the ability of IL-17A to promote fibrosis may be context specific. Lung transplant patients who develop BOS have increased IL-17A in BALF³². In allogeneic BMT mice, IFN- γ suppresses the production of IL-17A which is responsible for severe acute IPS³³. More recently, Varelias et al. demonstrated local IL-6 secretion in the absence of IFN- γ drives expansion of donor alloantigen-specific T_H17 cells to promote acute IPS development in both murine models and human HSCT patients³⁴. However, the role of IL-17A in development of fibrosis during the chronic phase of IPS has not yet been investigated. Here we identified a critical role for IL-17A in viral-driven lung fibrosis and pneumonitis post-HSCT. We found the increased levels of IL-17A in BMT mice directly contribute to fibrosis by stimulating proliferation and extracellular matrix synthesis in mesenchymal cells. We also considered the possibility that the T_H17 response was promoting the development of pneumonitis and fibrosis via the recruitment of neutrophils to the lung. We observed a 4-fold increase in neutrophils in the lung at 7 dpi, but there were no significant differences between BMT and non-BMT lungs analyzed at 10 dpi and afterwards (Supplementary Figure 3a online). Furthermore, administration of neutrophil specific depletion antibodies against Ly-6G³⁵ did not protect BMT mice from pneumonitis and pulmonary fibrosis at 21 dpi (Supplementary Figure 3b online).

Consistent with the skewing of T_H17 differentiation, we found that lung APCs in BMT mice produce more pro-T_H17 response cytokines and fewer T_H1 promoting cytokines with the exception of IL-12 (Figure 6a–b). The BMT APCs show little evidence of cytokine alteration in the absence of infection (Supplementary Figure 4a–b online) suggesting that γ HV-68 is actively contributing to this phenotype. Since BMT mice have higher early viral loads, we asked if different viral loads will contribute to the change of cytokine production

by the APCs. When infecting BMT and non-BMT APCs *ex vivo* with the same high dose (MOI=1) of γ HV-68, BMT APCs still secrete higher levels of T_H17 promoting cytokines than non-BMT DCs, suggesting an intrinsic alteration to the APCs in BMT mice. These data also suggest that IL-12 production by BMT APCs, accompanied with low levels of IFN- γ and high pro-T_H17 cytokines, is insufficient to promote viral-specific T_H1 responses. The CD4⁺ T cells themselves may also contribute to the skewing of T cell differentiation. The process of BMT induces changes in repopulating T cells that may favor T_H17 as opposed to T_H1 differentiation. Support for an altered T cell phenotype in BMT mice comes from the observation that BMT T cells do not proliferate well in a mixed lymphocyte response assay¹³. Thus the influence of BMT on T cell phenotype is a complex process and may involve not only lung APCs but also intrinsic T cell differences.

Adoptive transfer of primed lung APCs from normal mice into BMT mice can correct the T_H1/T_H17 balance after γ HV-68 infection, but adoptive transfer of APCs from BMT lungs into normal mice is not able to increase the level of T_H17 cells, likely due to the fact that the recipient mice still have endogenous non-BMT APCs available. Lung DCs include four main subsets: in an uninfected lung there are CD11b⁺ conventional DCs, CD103⁺ conventional DCs and plasmacytoid DCs, while upon inflammation, inflammatory monocyte-derived DCs are recruited to the lung³⁶. It has been reported that T_H17 cell responses are induced by inflammatory DCs³⁷ and CD103⁺ CD11b⁺ tissue-resident DCs^{38, 39}. The major APCs in our adoptive transfer studies were CD11b⁺ conventional myeloid DCs, but a limitation to our study is that the transferred cell population was a mixture of APC types. How non-BMT APCs overpower BMT APCs in guiding CD4⁺ T helper cell differentiation is not yet understood. When BMT lung APCs are adoptively transferred into non-BMT mice, the high levels of IFN- γ in non-BMT mice may work to suppress the pro-T_H17 effects of BMT lung APCs through suppression of their expression of IL-6^{33, 34}.

Prostaglandin E₂ (PGE₂) has previously been shown to promote T_H1 to T_H17 skewing by DCs^{40, 41}. PGE₂ can stimulate bone marrow-derived DCs to produce IL-23 and suppress IL-12 and thus promote T_H17 differentiation and maintenance^{40, 42-44}. Syngeneic BMT mice overexpress PGE₂ in the lungs both before and after viral infection^{13, 45}. However, inhibition of prostaglandin synthesis using indomethacin post-BMT did not alter clearance of lytic virus¹³ and we now confirm that use of PGE₂ synthase-deficient mice⁴⁶ as BMT donors and/or recipients has no impact on T_H1/T_H17 balance or development of pneumonitis and fibrosis (Supplementary Figure 5a-d online); however, it remains a formal possibility that other prostaglandins may be involved.

In summary, our data suggest preceding viral infections may be responsible for the later development of lung pathology in some HSCT recipients. Our mouse model of viral infection in BMT mice develops features of pneumonitis and fibrosis that are also noted in diseases like IPS, COP and BOS. This is consistent with previous clinical studies which suggest that a preceding respiratory viral infection may predict eventual development of lung pathology^{9, 10}. In contrast to these observations however, are recent data from cytomegalovirus (CMV) prophylaxis studies that have not demonstrated benefit for prophylactic therapy versus therapy initiated once viral replication is detected⁴⁷ in

prevention of endstage CMV disease and death. Right now, it is hard to know whether prophylaxis against a single organism can be effective, or whether new therapies are needed that can be used earlier post-transplant. Recently, sensitive testing of banked BAL fluid from IPS patients revealed a variety of previously unidentified pathogens in >56% of the total cases, with HHV6 being found most frequently⁸. Additionally, a trial of a new anti-CMV therapy with reduced bone marrow toxicity allowing treatment to start sooner post-HSCT, demonstrated that many patients were positive for viral replication before prophylactic therapy is routinely started^{48, 49}. Excitingly, this drug, letermovir, did show promise in limiting CMV end-stage disease. A final hopeful note is that our data, along with accumulating evidence from other studies mentioned above suggest that neutralization of IL-17A may be an effective therapy to limit pneumonitis and fibrosis even when started late after disease onset.

Methods

Mouse strains

C57BL/6J mice were purchased from the Jackson Laboratory (Bar Harbor, ME). B6.*Il-17a*^{-/-} mice²⁰ and inducible prostaglandin synthase deficient mice (*mPGEs*^{-/-})⁴⁶ have been previously described and were bred in the animal facility of the University of Michigan, Ann Arbor, MI. Experiments were approved by the University of Michigan Committee on the Use and Care of Animals.

Syngeneic BMT

Recipient WT or B6.*Il-17a*^{-/-} mice were treated with 13 Gy total body irradiation (split dose) using a ¹³⁷Cs irradiator, followed by tail vein injection of 5×10^6 whole bone marrow cells from WT or B6. *Il-17a*^{-/-} mice. Chimeras were infected with γ HV-68 at the fifth week after BMT, when total numbers of hematopoietic cells were fully reconstituted in the lungs and spleen¹⁴.

γ HV-68 infection and plaque assays

Non-BMT or BMT mice were infected with 5×10^4 pfu of murine γ HV-68 (VR-1465, ATCC, Manassas, VA), γ HV-68-H2bYFP¹⁵ or v-cyclin deficient γ HV-68¹⁸ intranasally after being anesthetized with ketamine and xylazine. To quantify lytic virus, right lungs were harvested and homogenized in 1 ml complete media. Supernatants were diluted and inoculated onto 3T12 cells (ATCC, Manassas, VA); plaques were enumerated 7 days later.

Lung cell preparation and flow cytometry

Single cell suspensions of leukocytes were prepared from whole lungs by collagenase digestion for flow cytometry as described previously¹³. Briefly, each minced lung was incubated in 15 ml of complete media with 1 mg/ml collagenase (Boehringer Mannheim Biochemical, Chicago, IL), and 17 U/ml DNase I (Sigma-Aldrich, St. Louis, MO) for 30 minutes at 37°C. The digested tissue was drawn through the bore of a 10-ml syringe repeatedly, and filtered through 100 μ m mesh. Cells were stimulated with PMA (0.05 mg/ml; Sigma-Aldrich, St. Louis, MO) and ionomycin (0.75 mg/ml; Sigma-Aldrich, St. Louis, MO) for 4 h in the presence of GolgiStop protein transport inhibitor (BD

Pharmingen, San Jose, CA) before intracellular cytokine staining. An aliquot of 1×10^6 cells was first blocked by anti-CD16/CD32 (Fc block; BD Pharmingen, San Jose, CA) antibodies and then stained using fluorochrome-conjugated antibodies against CD45, CD4, IL-17A, IL-4 or IFN- γ (BD Pharmingen, San Jose, CA). For characterization of lung APCs, flow cytometry was performed using antibodies specific for CD11c (N418), CD103 (2E7), I-A $_b$ (AF6-120.1), and CD68 (FA-11), all from BioLegend (San Diego, CA); CD11b (M1/70, BD Pharmingen); and Ly6C (HK1.4) and F4/80 (BM8) from eBioscience (San Diego, CA). The FITC channel was used to detect autofluorescence of alveolar macrophages.

Lung APC adoptive transfer

Single cell suspensions were prepared from whole lungs and mediastinal lymph nodes by collagenase digestion. Macrophages were reduced from the suspensions by 90-min adherence on tissue culture plastic. CD11c $^+$ cells were then positively selected by using anti-mouse CD11c magnetic microbeads and columns (Miltenyi Biotec, Auburn CA). A total of 5×10^5 CD11c $^+$ lung APCs were injected into recipients via tail vein.

***In vivo* neutralization of IL-17A**

Rabbit polyclonal antibodies against mouse IL-17A were generated and specificity of the antibodies was tested using a direct ELISA to IL-17A as well as other IL-17 family members⁵⁰. A dose of 2.5 mg of purified polyclonal anti-mouse IL-17A or rabbit IgG isotype was injected intraperitoneally at designated time points.

Cidofovir treatment

Cidofovir (Mylan, Institutional LLC) was administered subcutaneously at a dose of 25 mg/kg of body weight. Mice were treated for 2 consecutive days starting at the designated date and then were injected in every 3 days until 21 dpi.

Lung section staining and microscopy

For immunofluorescence staining, frozen lung sections were fixed in 3.7% formaldehyde, followed by blocking with 1% BSA in PBS, and stained with a chicken anti-GFP primary antibody (Abcam, Cambridge, MA) and an Alexa Fluor 488 conjugated goat anti-chicken secondary antibody (Life technology, Carlsbad, CA). Images were collected on a Zeiss ApoTome fluorescent microscope using AxioVision software. For hematoxylin and eosin (H&E) staining or Masson's trichrome staining, whole lungs were inflated and fixed with 10% buffered formalin, dehydrated by ethanol and embedded in paraffin. Sections were cut at a thickness of 3 μ m, mounted on glass slides and stained using H&E or Masson's trichrome. Images were taken on a Olympus BX-51 microscope by a DP-70 camera.

Quantitative RT-PCR

The relative amount of mRNA for target genes was assayed by real-time RTPCR using thermocycler ABI Prism 7000 (Applied Biosystems, Inc., Foster City, CA) using a previously described protocol⁴⁵. Gene-specific primers and probes (Table 1) were designed using Primer Express software (Applied Biosystems, Inc.).

Enzyme-linked immunosorbent assay (ELISA)

ELISA for active TGF β was performed using R&D Systems kits according to manufacturer's instructions.

Histologic scores

Histologic sections stained with H&E and trichrome were scored in a blinded fashion by a lung pathologist (Dr. Konopka) as described previously¹². Lungs were scored for severity of fibrosis, perivascular inflammation, peripheral inflammation, presence or absence of foamy alveolar macrophages and intra-alveolar fibrin. The scores for each factor were added to give a pathology score, with 11 indicating the most severe phenotype.

Mesenchymal cell assays

Mesenchymal cells were isolated from lung minces of non-BMT mice following 2 weeks of culture. Proliferation assays utilized 5000 mesenchymal cells/well in 96 well plates in serum-free media treated with the indicated concentrations of IL-17A for 48 h prior to addition of ³H-thymidine and determination of radiolabeled DNA in the nucleus as a measure of cellular proliferation. For measurement of extracellular matrix, 4×10^5 mesenchymal cells were cultured in serum-free media in the presence of IL-17A for 48 or 72 h prior to the collection of total cellular RNA and analysis of collagen 1, collagen 3 and fibronectin by real-time RT-PCR.

Statistical analysis

When groups of 2 were compared, student's *t*-tests were used to determine significance; when groups of 3 or more were compared, ANOVA was utilized with a Tukey's multiple comparisons test to determine significance.

Supplementary Material

Refer to Web version on PubMed Central for supplementary material.

Acknowledgements

This work was supported by NIH grant AI117229 and HL115618 awarded to BBM. XZ and SG were supported by T32HL07749. XZ was also supported by Post-doctoral translational scholar grant from MICHR 2UL1TR000433. SC was supported by T32 AI007413 at the time of this work when she was at the University of Michigan. We are also grateful to Dr. Sam Speck from Emory University who provided the γ HV-68-H2bYFP virus for these studies.

References

1. Afessa B, Peters SG. Major complications following hematopoietic stem cell transplantation. *Semin Respir Crit Care Med.* 2006; 27(3):297–309. [PubMed: 16791762]
2. Soubani AO, Pandya CM. The spectrum of noninfectious pulmonary complications following hematopoietic stem cell transplantation. *Hematol Oncol Stem Cell Ther.* 2010; 3(3):143–157. [PubMed: 20890072]
3. Passweg JR, Baldomero H, Peters C, Gaspar HB, Cesaro S, Dreger P, et al. Hematopoietic SCT in Europe: data and trends in 2012 with special consideration of pediatric transplantation. *Bone Marrow Transplant.* 2014; 49(6):744–750. [PubMed: 24637898]

4. Wingard JR, Hsu J, Hiemenz JW. Hematopoietic stem cell transplantation: an overview of infection risks and epidemiology. *Infect Dis Clin North Am.* 2010; 24(2):257–272. [PubMed: 20466269]
5. Yoshihara S, Yanik G, Cooke KR, Mineishi S. Bronchiolitis obliterans syndrome (BOS), bronchiolitis obliterans organizing pneumonia (BOOP), and other late-onset noninfectious pulmonary complications following allogeneic hematopoietic stem cell transplantation. *Biol Blood Marrow Transplant.* 2007; 13(7):749–759. [PubMed: 17580252]
6. Uhlving HH, Andersen CB, Christensen IJ, Gormsen M, Pedersen KD, Buchvald F, et al. Biopsy-Verified Bronchiolitis Obliterans and Other Noninfectious Lung Pathologies after Allogeneic Hematopoietic Stem Cell Transplantation. *Biol Blood Marrow Transplant.* 2014; 21(3):531–538. [PubMed: 25498923]
7. Panoskaltsis-Mortari A, Griese M, Madtes DK, Belperio JA, Haddad IY, Folz RJ, et al. An official American Thoracic Society research statement: noninfectious lung injury after hematopoietic stem cell transplantation: idiopathic pneumonia syndrome. *Am J Respir Crit Care Med.* 2011; 183(9):1262–1279. [PubMed: 21531955]
8. Seo S, Renaud C, Kuypers JM, Chiu CY, Huang ML, Samayoa E, et al. Idiopathic pneumonia syndrome after hematopoietic cell transplantation: evidence of occult infectious etiologies. *Blood.* 2015; 125(24):3789–3797. [PubMed: 25918347]
9. Erard V, Chien JW, Kim HW, Nichols WG, Flowers ME, Martin PJ, et al. Airflow decline after myeloablative allogeneic hematopoietic cell transplantation: the role of community respiratory viruses. *J Infect Dis.* 2006; 193(12):1619–1625. [PubMed: 16703503]
10. Versluys AB, Rossen JW, van Ewijk B, Schuurman R, Bierings MB, Boelens JJ. Strong association between respiratory viral infection early after hematopoietic stem cell transplantation and the development of life-threatening acute and chronic alloimmune lung syndromes. *Biol Blood Marrow Transplant.* 2010; 16(6):782–791. [PubMed: 20060053]
11. Moore BB, Moore TA. Viruses in idiopathic pulmonary fibrosis: Etiology and Exacerbation. *Annals of the Am Thorac Soc.* 2015 (**in press**).
12. Coomes SM, Farmen S, Wilke CA, Laouar Y, Moore BB. Severe gammaherpesvirus-induced pneumonitis and fibrosis in syngeneic bone marrow transplant mice is related to effects of transforming growth factor-beta. *Am J Pathol.* 2011; 179(5):2382–2396. [PubMed: 21924228]
13. Coomes SM, Wilke CA, Moore TA, Moore BB. Induction of TGF-beta 1, not regulatory T cells, impairs antiviral immunity in the lung following bone marrow transplant. *J Immunol.* 2010; 184(9):5130–5140. [PubMed: 20348421]
14. Hubbard LL, Ballinger MN, Wilke CA, Moore BB. Comparison of conditioning regimens for alveolar macrophage reconstitution and innate immune function post bone marrow transplant. *Experimental lung research.* 2008; 34(5):263–275. [PubMed: 18465404]
15. Collins CM, Speck SH. Tracking murine gammaherpesvirus 68 infection of germinal center B cells in vivo. *PloS one.* 2012; 7(3):e33230. [PubMed: 22427999]
16. Vannella KM, Luckhardt TR, Wilke CA, van Dyk LF, Toews GB, Moore BB. Latent herpesvirus infection augments experimental pulmonary fibrosis. *Am J Respir Crit Care Med.* 2010; 181(5):465–477. [PubMed: 20185751]
17. Mora AL, Torres-Gonzalez E, Rojas M, Xu J, Ritzenthaler J, Speck SH, et al. Control of virus reactivation arrests pulmonary herpesvirus-induced fibrosis in IFN-gamma receptor-deficient mice. *Am J Respir Crit Care Med.* 2007; 175(11):1139–1150. [PubMed: 17363768]
18. van Dyk LF, Virgin HW, Speck SH. The murine gammaherpesvirus 68 v-cyclin is a critical regulator of reactivation from latency. *Journal of virology.* 2000; 74(16):7451–7461. [PubMed: 10906198]
19. Lea AP, Bryson HM. Cidofovir. *Drugs.* 1996; 52(2):225–230. discussion 231. [PubMed: 8841740]
20. Nakae S, Komiyama Y, Nambu A, Sudo K, Iwase M, Homma I, et al. Antigen-specific T cell sensitization is impaired in IL-17-deficient mice, causing suppression of allergic cellular and humoral responses. *Immunity.* 2002; 17(3):375–387. [PubMed: 12354389]
21. Lukacs NW, Smit JJ, Mukherjee S, Morris SB, Nunez G, Lindell DM. Respiratory virus-induced TLR7 activation controls IL-17-associated increased mucus via IL-23 regulation. *J Immunol.* 2010; 185(4):2231–2239. [PubMed: 20624950]

22. Yao Z, Fanslow WC, Seldin MF, Rousseau AM, Painter SL, Comeau MR, et al. Herpesvirus Saimiri encodes a new cytokine, IL-17, which binds to a novel cytokine receptor. *Immunity*. 1995; 3(6):811–821. [PubMed: 877726]
23. Holt PG, Batty JE. Alveolar macrophages. V. Comparative studies on the antigen presentation activity of guinea-pig and rat alveolar macrophages. *Immunology*. 1980; 41(2):361–366. [PubMed: 6160094]
24. Doherty PC, Christensen JP, Belz GT, Stevenson PG, Sangster MY. Dissecting the host response to a gamma-herpesvirus. *Philosophical transactions of the Royal Society of London Series B, Biological sciences*. 2001; 356(1408):581–593. [PubMed: 11313013]
25. Travis EL, Down JD, Holmes SJ, Hobson B. Radiation pneumonitis and fibrosis in mouse lung assayed by respiratory frequency and histology. *Radiat Res*. 1980; 84(1):133–143. [PubMed: 7454976]
26. Wilson MS, Madala SK, Ramalingam TR, Gochuico BR, Rosas IO, Cheever AW, et al. Bleomycin and IL-1beta-mediated pulmonary fibrosis is IL-17A dependent. *J Exp Med*. 2010; 207(3):535–552. [PubMed: 20176803]
27. Mi S, Li Z, Yang HZ, Liu H, Wang JP, Ma YG, et al. Blocking IL-17A promotes the resolution of pulmonary inflammation and fibrosis via TGF-beta1-dependent and -independent mechanisms. *J Immunol*. 2011; 187(6):3003–3014. [PubMed: 21841134]
28. Lei L, Zhong XN, He ZY, Zhao C, Sun XJ. IL-21 Induction of CD4+ T Cell Differentiation into Th17 Cells Contributes to Bleomycin-Induced Fibrosis in Mice. *Cell Biol Int*. 2014; 39(4):388–399. [PubMed: 25492803]
29. Francois A, Gombault A, Villeret B, Alsaleh G, Fanny M, Gasse P, et al. B cell activating factor is central to bleomycin- and IL-17-mediated experimental pulmonary fibrosis. *J Autoimmun*. 2014; 56:1–11. [PubMed: 25441030]
30. Simonian PL, Roark CL, Wehrmann F, Lanham AK, Diaz del Valle F, Born WK, et al. Th17-polarized immune response in a murine model of hypersensitivity pneumonitis and lung fibrosis. *J Immunol*. 2009; 182(1):657–665. [PubMed: 19109199]
31. Lo Re S, Dumoutier L, Couillin I, Van Vyve C, Yakoub Y, Uwambayinema F, et al. IL-17A-producing gammadelta T and Th17 lymphocytes mediate lung inflammation but not fibrosis in experimental silicosis. *J Immunol*. 2010; 184(11):6367–6377. [PubMed: 20421647]
32. Vanaudenaerde BM, De Vleeschauwer SI, Vos R, Meyts I, Bullens DM, Reynders V, et al. The role of the IL23/IL17 axis in bronchiolitis obliterans syndrome after lung transplantation. *Am J Transplant*. 2008; 8(9):1911–1920. [PubMed: 18786233]
33. Mauermann N, Burian J, von Garnier C, Dirnhofner S, Germano D, Schuett C, et al. Interferon-gamma regulates idiopathic pneumonia syndrome, a Th17+CD4+ T-cell-mediated graft-versus-host disease. *Am J Respir Crit Care Med*. 2008; 178(4):379–388. [PubMed: 18511701]
34. Varelias A, Gartlan KH, Kreijveld E, Olver SD, Lor M, Kuns RD, et al. Lung parenchyma-derived IL-6 promotes IL-17A-dependent acute lung injury after allogeneic stem cell transplantation. *Blood*. 2015; 125(15):2435–2444. [PubMed: 25673640]
35. Daley JM, Thomay AA, Connolly MD, Reichner JS, Albina JE. Use of Ly6G-specific monoclonal antibody to deplete neutrophils in mice. *Journal of leukocyte biology*. 2008; 83(1):64–70. [PubMed: 17884993]
36. Neyt K, Lambrecht BN. The role of lung dendritic cell subsets in immunity to respiratory viruses. *Immunol Rev*. 2013; 255(1):57–67. [PubMed: 23947347]
37. Segura E, Touzot M, Bohineust A, Cappuccio A, Chiochia G, Hosmalin A, et al. Human inflammatory dendritic cells induce Th17 cell differentiation. *Immunity*. 2013; 38(2):336–348. [PubMed: 23352235]
38. Schlitzer A, McGovern N, Teo P, Zelante T, Atarashi K, Low D, et al. IRF4 transcription factor-dependent CD11b+ dendritic cells in human and mouse control mucosal IL-17 cytokine responses. *Immunity*. 2013; 38(5):970–983. [PubMed: 23706669]
39. Persson EK, Uronen-Hansson H, Semmrich M, Rivollier A, Hagerbrand K, Marsal J, et al. IRF4 transcription-factor-dependent CD103(+)/CD11b(+) dendritic cells drive mucosal T helper 17 cell differentiation. *Immunity*. 2013; 38(5):958–969. [PubMed: 23664832]

40. Sheibanie AF, Yen JH, Khayrullina T, Emig F, Zhang M, Tuma R, et al. The proinflammatory effect of prostaglandin E2 in experimental inflammatory bowel disease is mediated through the IL-23--> IL-17 axis. *J Immunol.* 2007; 178(12):8138–8147. [PubMed: 17548652]
41. Boniface K, Bak-Jensen KS, Li Y, Blumenschein WM, McGeachy MJ, McClanahan TK, et al. Prostaglandin E2 regulates Th17 cell differentiation and function through cyclic AMP and EP2/EP4 receptor signaling. *J Exp Med.* 2009; 206(3):535–548. [PubMed: 19273625]
42. Sheibanie AF, Tadmori I, Jing H, Vassiliou E, Ganea D. Prostaglandin E2 induces IL-23 production in bone marrow-derived dendritic cells. *FASEB J.* 2004; 18(11):1318–1320. [PubMed: 15180965]
43. Khayrullina T, Yen JH, Jing H, Ganea D. In vitro differentiation of dendritic cells in the presence of prostaglandin E2 alters the IL-12/IL-23 balance and promotes differentiation of Th17 cells. *J Immunol.* 2008; 181(1):721–735. [PubMed: 18566439]
44. Poloso NJ, Urquhart P, Nicolaou A, Wang J, Woodward DF. PGE2 differentially regulates monocyte-derived dendritic cell cytokine responses depending on receptor usage (EP2/EP4). *Mol Immunol.* 2013; 54(3–4):284–295. [PubMed: 23337716]
45. Ballinger MN, Aronoff DM, McMillan TR, Cooke KR, Olkiewicz K, Toews GB, et al. Critical role of prostaglandin E2 overproduction in impaired pulmonary host response following bone marrow transplantation. *J Immunol.* 2006; 177(8):5499–5508. [PubMed: 17015736]
46. Trebino CE, Stock JL, Gibbons CP, Naiman BM, Wachtmann TS, Umland JP, et al. Impaired inflammatory and pain responses in mice lacking an inducible prostaglandin E synthase. *Proceedings of the National Academy of Sciences of the United States of America.* 2003; 100(15):9044–9049. [PubMed: 12835414]
47. Boeckh M, Nichols WG, Chemaly RF, Papanicolaou GA, Wingard JR, Xie H, et al. Valganciclovir for the prevention of complications of late cytomegalovirus infection after allogeneic hematopoietic cell transplantation: a randomized trial. *Annals of internal medicine.* 2015; 162(1):1–10. [PubMed: 25560711]
48. Griffiths PD, Emery VC. Taming the transplantation troll by targeting terminase. *The New England Journal of Medicine.* 2014; 370(19):1844–1846. [PubMed: 24806164]
49. Chemaly RF, Ullmann AJ, Stoelben S, Richard MP, Bornhauser M, Groth C, et al. Letermovir for cytomegalovirus prophylaxis in hematopoietic-cell transplantation. *The New England Journal of Medicine.* 2014; 370(19):1781–1789. [PubMed: 24806159]
50. Mukherjee S, Lindell DM, Berlin AA, Morris SB, Shanley TP, Hershenson MB, et al. IL-17-induced pulmonary pathogenesis during respiratory viral infection and exacerbation of allergic disease. *Am J Pathol.* 2011; 179(1):248–258. [PubMed: 21703407]

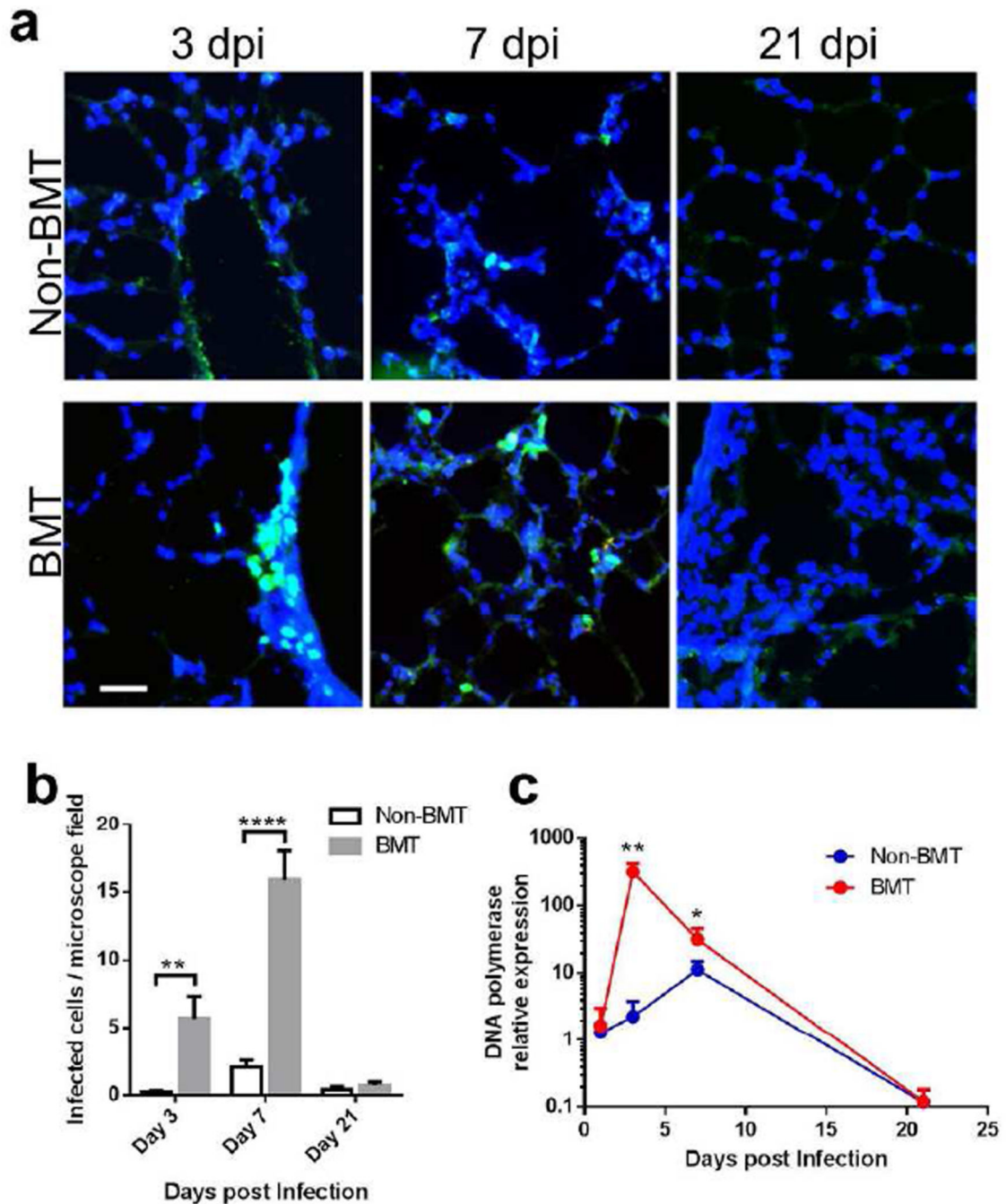


Figure 1. BMT mice cannot restrict gammaherpesvirus lytic replication

(a) Representative lung sections from $n=3$ syngeneic BMT C57BL/6J mice or age-matched non-BMT mice infected with 5×10^4 pfu γ HV-68-H2bYFP intranasally and analyzed by histology at 3, 7 or 21 dpi (bars = 40 μ m, same magnification for the images). H2bYFP expressed in viral infected cells was detected by a cross-reactive FITC conjugated anti-GFP antibody (green). DAPI nuclear counterstains are blue. (b) YFP positive virus infected cell count per microscope field under 1000 \times magnification (mean + SEM, $n = 10$). A typical field has about 250 cells in total. Data are pooled from two independent experiments. ** $P <$

0.01 and **** $P < 0.0001$. (c) γ HV-68 lytic replication in BMT or non-BMT mice at designated time points postinfection as measured by relative mRNA abundance of viral DNA polymerase (mean + SEM, n = 5). * $P < 0.05$ and ** $P < 0.01$, **** $P < 0.0001$. Similar results were obtained in two additional experiments.

Author Manuscript

Author Manuscript

Author Manuscript

Author Manuscript

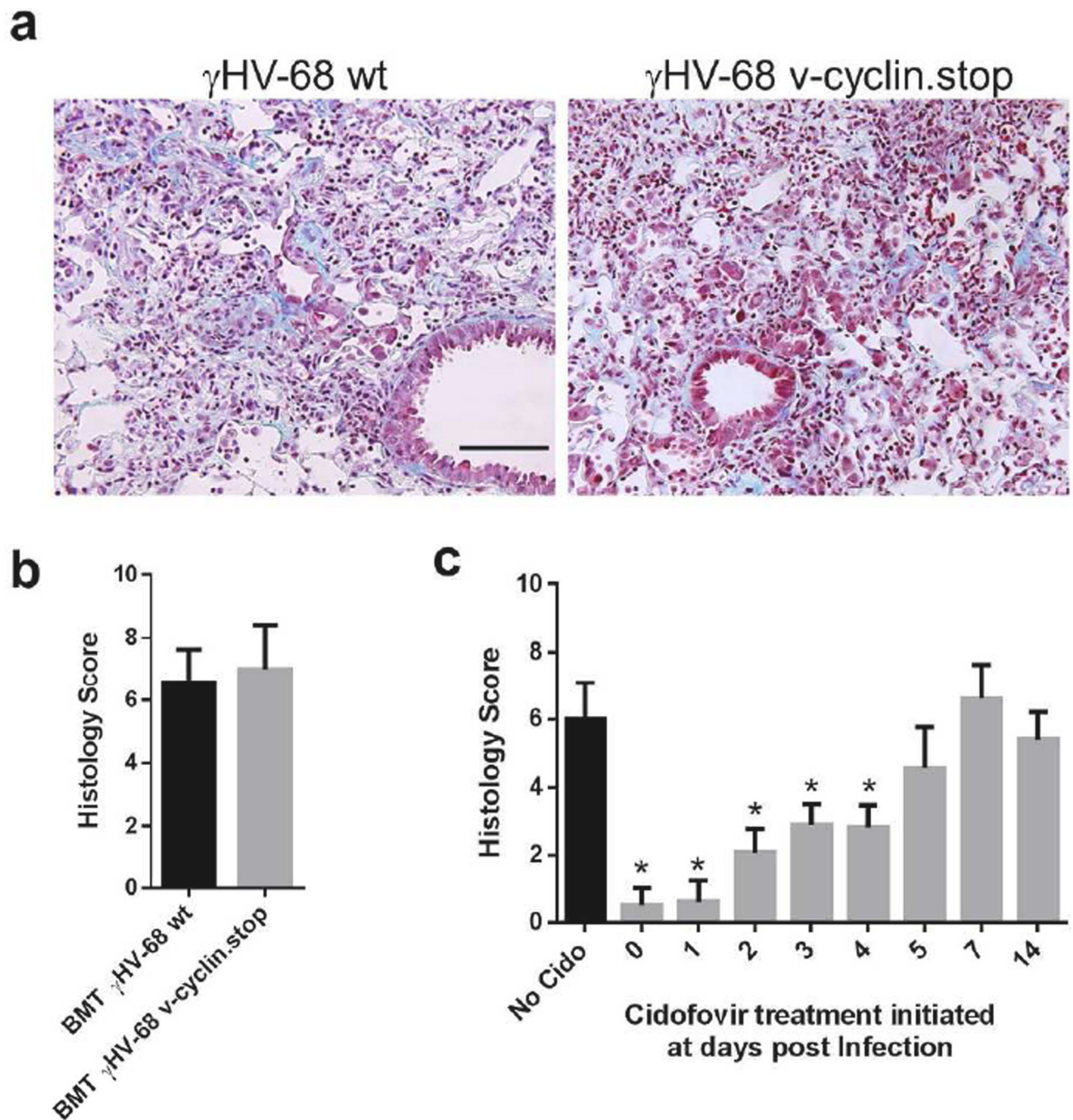


Figure 2. Viral reactivation is not required for development of pneumonitis and lung fibrosis in BMT mice

(a) Representative lung sections from BMT mice infected with either a γ HV-68 mutant containing a stop codon within ORF 72 (v-cyclin.stop) or the wild type virus at 21 dpi. The lung sections were stained with Masson's trichrome and blue staining represents deposition of collagen. Same magnification for both images (bar = 100 μ m), (b) The average histology scores of lung sections from v-cyclin. stop or wild type virus infected BMT mice at 21 dpi (mean + SEM, n = 5). Lung sections were scored on an 11 point scale as in Methods. (c) Average histology scores of lung sections from γ HV-68 infected BMT mice with or without

cidofovir treatment starting at designated days post viral infection (mean + SEM, n = 5). Cidofovir was administered subcutaneously at a dose of 25 mg/kg of body weight. Mice were treated with cidofovir for 2 consecutive days and then were injected in every 3 days until 21 dpi. * $P < 0.05$. Similar results were obtained in two additional experiments.

Author Manuscript

Author Manuscript

Author Manuscript

Author Manuscript

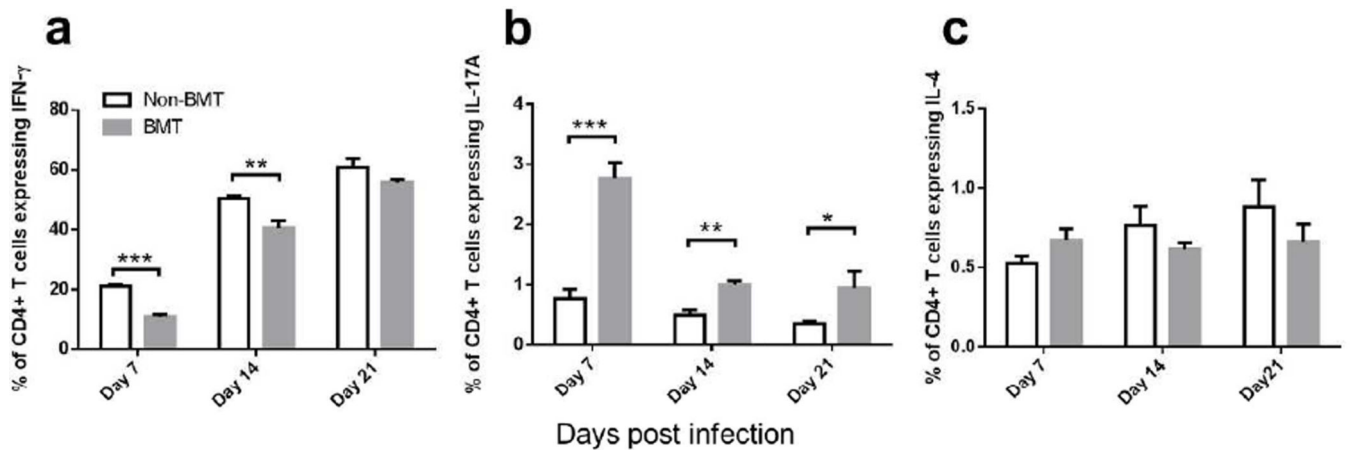


Figure 3. Increased T_H17 cells and decreased T_H1 cells are found in BMT mice post γ HV-68 infection

Single cell suspensions were prepared by collagenase digestion of whole lungs of non-BMT control or BMT mice at 7, 14 or 21 dpi with γ HV-68. Cells were then stimulated with PMA and ionomycin and analyzed by flow cytometry. CD45⁺ CD4⁺ cells were gated. (a) Percent of CD4⁺ cells that express IFN- γ (T_H1 cells); (b) percent of CD4⁺ cells that express IL-17A (T_H17 cells); (c) percent of CD4⁺ cells that express IL-4 (T_H2 cells). * $P < 0.05$, ** $P < 0.01$, *** $P < 0.001$. Data are pooled from two independent experiments (Mean + SEM, n = 7).

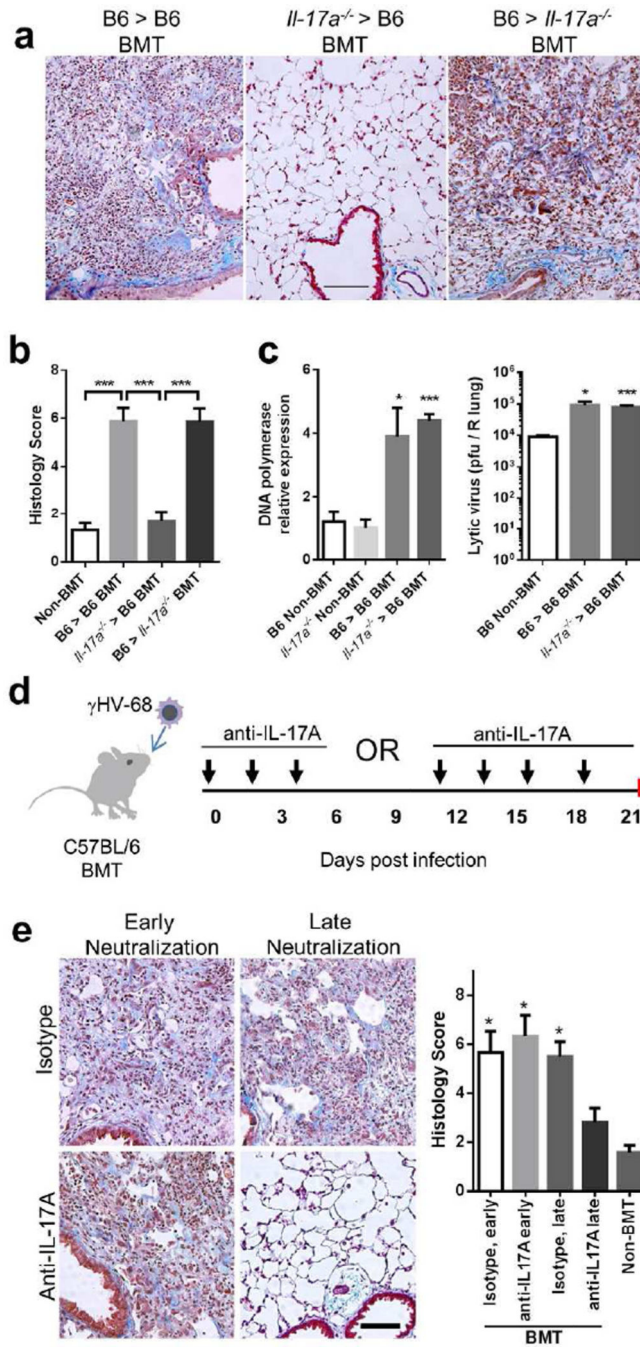


Figure 4. Bone marrow-derived IL-17A is required for development of pneumonitis and fibrosis in γ HV-68 infected BMT mice

(a) Representative Masson's trichrome staining of lung sections from WT and *Il-17a*^{-/-} BMT chimeric mice infected with γ HV-68 virus at 21 dpi. The blue staining represents deposition of collagen. Same magnification for all images (bar = 100 μ m). (b) The average histology scores of lung sections from γ HV-68 infected non-BMT or BMT mice as described in (a) at 21 dpi (mean + SEM, n = 5). (c) Lytic replication of γ HV-68 in non-BMT WT or *Il-17a*^{-/-}, and in WT recipients of WT grafts or *Il-17a*^{-/-} grafts at 7 dpi. Left, mRNA abundance of viral DNA polymerase as measured by RT-PCR (mean + SEM, n = 5); right,

the number of lytic virus per right lung was directly measured by plaque assay (mean + SEM, n = 5). Each group was compared to WT non-BMT mice. (d) A scheme of γ HV-68 infection and subsequent administration of IL-17A neutralization antibodies in WT BMT mice. (e) The requirement of IL-17A for development of pneumonitis and fibrosis in BMT mice during late stages. Left, representative Masson's trichrome staining of lung sections from antibody treated BMT mice at 21 dpi. BMT mice received anti-IL-17A antibodies or isotype treatment at early or late time points as shown in (d). The blue staining represents deposition of collagen. Right, average histology scores of lung sections from γ HV-68 infected non-BMT or BMT mice treated with anti-IL-17A antibodies or isotype (mean + SEM, n = 4). Each group was compared to BMT mice treated with anti-IL-17A antibodies at late time points. * $P < 0.05$ and *** $P < 0.001$. Similar results were seen in 2 additional experiments (a, b) or one additional experiment (c, e).

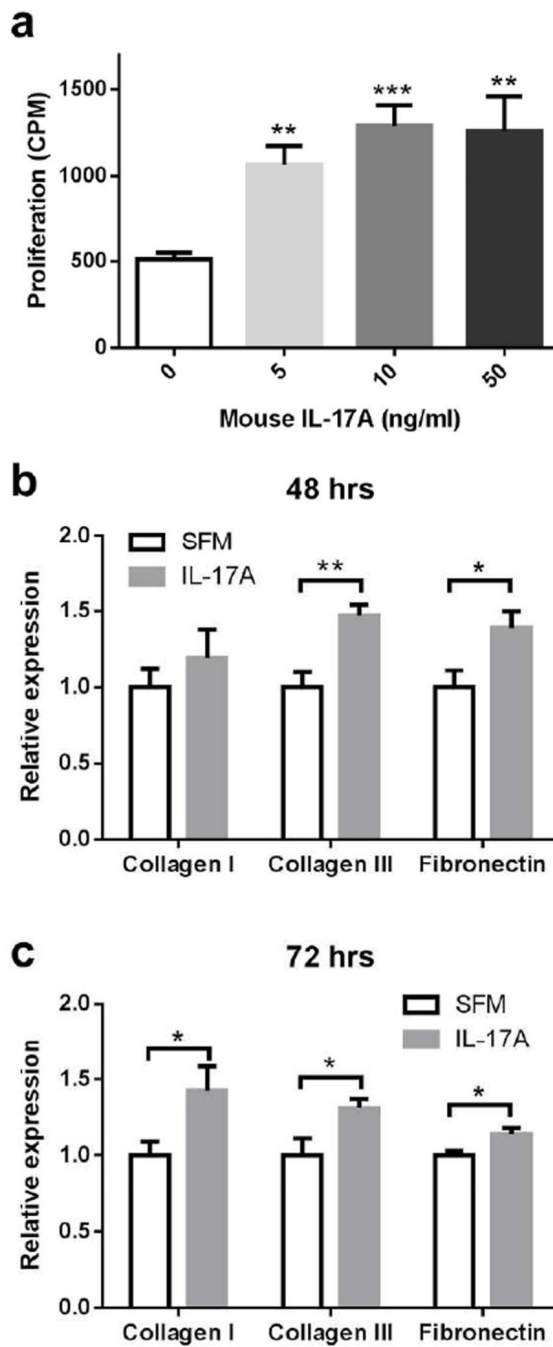


Figure 5. IL-17A directly activates lung mesenchymal cells

(a) Dose response of mouse primary lung mesenchymal cell proliferation to recombinant murine IL-17A *in vitro* as measured by uptake of ^3H -thymidine (mean + SEM, n = 10). Each group was compared to the cells with solvent only. (b) and (c) Mouse primary mesenchymal cell mRNA expression of collagens 1 and 3 and fibronectin in response to stimulation with 10 ng/ml recombinant murine IL-17A *in vitro* at 48 hours (b) and 72 hours (c). * $P < 0.05$, ** $P < 0.01$ and *** $P < 0.001$. Similar results were seen in 2 additional experiments.

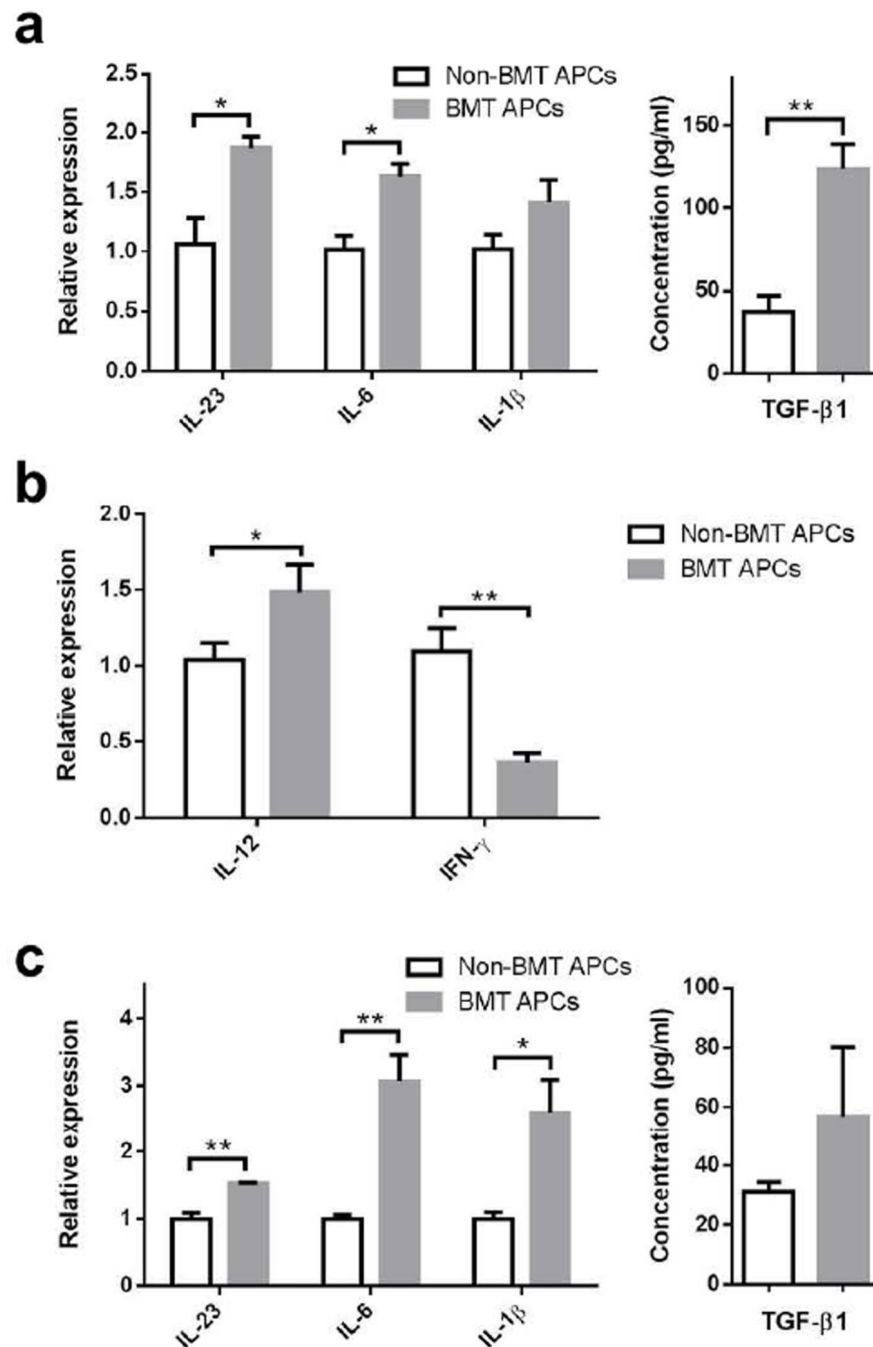


Figure 6. Altered cytokine expression in lung APCs from BMT mice in response to γ HV-68 infection

(a) Expression of IL-6, IL-23p19, IL-1 β , and TGF- β 1 in lung APCs from infected non-BMT or BMT mice. Lung CD11c⁺ enriched APCs were isolated from non-BMT or BMT mice at 7 dpi. A total of 2×10^6 lung APCs were seeded in a well of 24-well plate and re-stimulated with 0.25 MOI of γ HV-68 for 36 hours. Left, RT-PCR analysis of mRNA for IL-6, IL-23 and IL-1 β in lung APCs (mean + SEM, n = 4); Right, ELISA for TGF- β 1 in culture supernatant of lung APCs (mean + SEM, n = 4). (b) Expression of IL-12p35 and IFN- γ mRNA in same cells as in (a). (c) Expression of IL-6, IL-23, IL-1 β and TGF- β 1 in lung APCs from

uninfected non-BMT or BMT mice. Lung CD11c⁺ APCs were enriched from uninfected non-BMT or BMT mice and were stimulated with 1 MOI virus *ex vivo* for 24 hours. Left, RT-PCR analysis of mRNA of IL-6, IL-23 and IL-1 β in lung APCs; Right, ELISA for TGF- β 1 in culture supernatant of lung APCs (mean + SEM, n = 3).

Author Manuscript

Author Manuscript

Author Manuscript

Author Manuscript

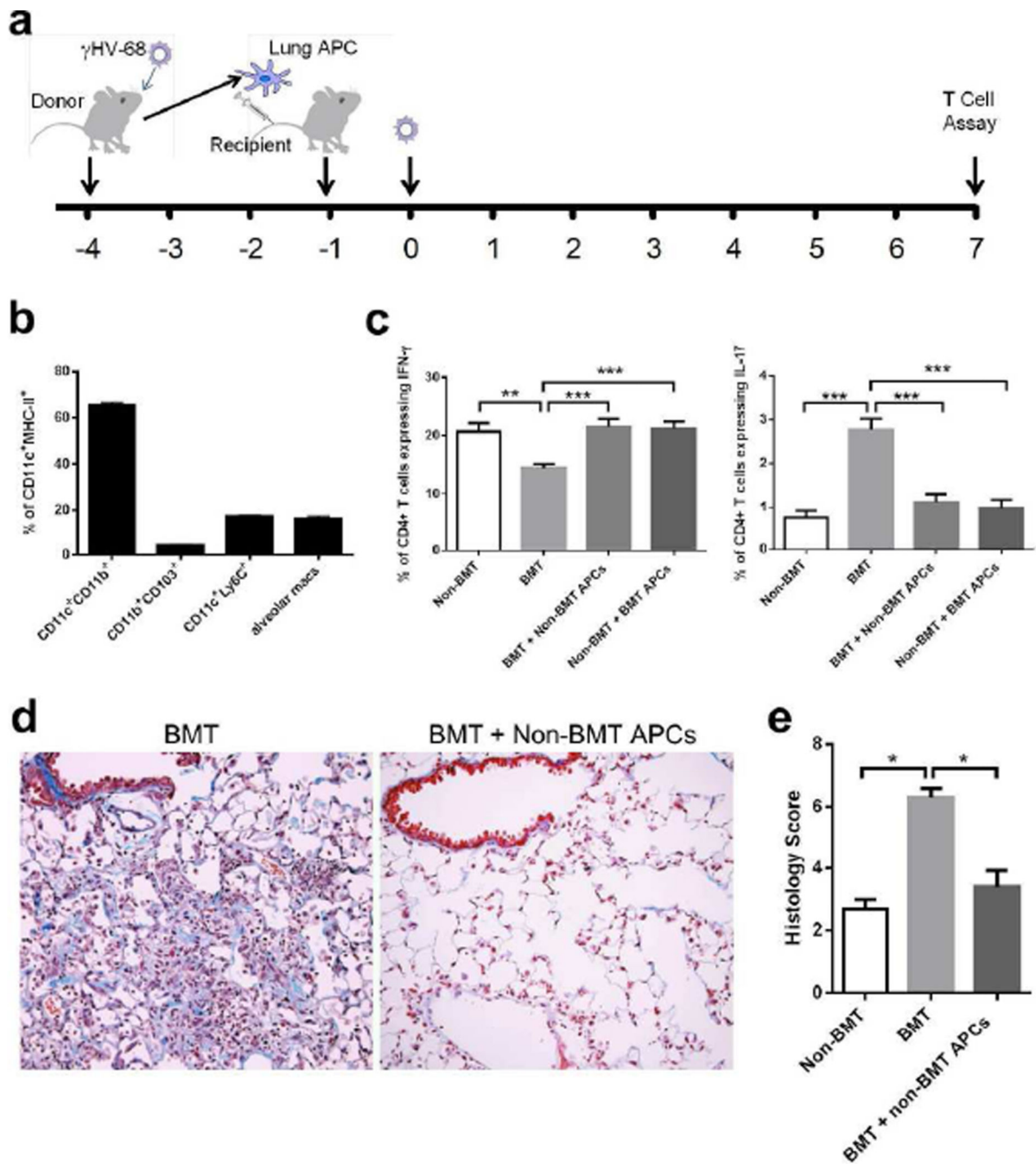


Figure 7. Lung APCs from non-BMT mice restore T_H1 and limit T_H17 response in BMT mice (a) A scheme of adoptive transfer of lung APCs and γ HV-68 infection. (b) Characterization of CD11c⁺ MHC class II⁺ cell population used for adoptive transfer. (c) The alteration of the percentage of CD4⁺ IFN- γ ⁺ T_H1 cells and CD4⁺ IL-17A⁺ T_H17 cells by adoptive transfer of lung APCs. Lung CD11c⁺ APCs were enriched by magnetic beads from viral-infected non-transplanted or BMT mice, and adoptively transferred into BMT mice or non-transplanted mice, respectively. Single cell suspensions were prepared at 7 dpi for PMA stimulation and flow cytometry analysis. Left, percent of CD4⁺ cells that express IFN- γ

(T_H1 cells, mean + SEM, n = 5); Right, percent of CD4+ cells that express IL-17A (T_H17 cells, mean + SEM, n = 5). (d) Representative Masson's trichrome staining on lung sections from BMT mice with or without adoptive transfer of primed non-BMT lung APCs at 21 dpi. The blue staining represents deposition of collagen. Same magnification was used for all images. (e) The average histology scores of lung sections from γ HV-68 infected non-BMT, BMT mice or BMT mice adoptively transferred with non-BMT lung APCs at 21 dpi (mean + SEM, n = 3). * $P < 0.05$, ** $P < 0.01$, *** $P < 0.001$. Similar results were obtained in two (b, d, e) or three (c) independent experiments.

Table 1

Primers and Probes for Semiquantitative Real-Time RT-PCR

Gene	Oligo	Primer sequence
DNA polymerase (ORF9)	Forward	5'-ACAGCAGCTGGCCATAAAGG-3'
	Reverse	5'-TCCTGCCCTGGAAAAGTGATG-3'
	Probe	5'-CCTCTGGAATGTTGCCTTGCCTCCA-3'
β -Actin	Forward	5'-CCGTGAAAAGATGACCCAGATC-3'
	Reverse	5'-CACAGCCTGGATGGCTACGT-3'
	Probe	5'-TTTGAGACCTTCAACACCCCAAGCCA-3'
Collagen I	Forward	5'-TGACTGGAAGAGCGGAGACT-3'
	Reverse	5'-GGTCTGACCTGTCTCCATGTTG-3'
	Probe	5'-CTGCAACCTGGACGCCATCAAGG-3'
Collagen III	Forward	5'-GGATCTGTCTTTGCGATGAC-3'
	Reverse	5GCTGTGGGCATATTGCACAA-3'
	Probe	5'-TGCCCAACCCAGAGATCCCATTT-3'
Fibronectin	Forward	5'-TCGAGCCCTGAGGATGGA-3'
	Reverse	5'-GTGCAAGGCAACCACACTGA-3'
	Probe	5'-CTGACGGCCTCAGGCCGG-3'
IL23 p19	Forward	5'-CTCCCTACTAGGACTCAGCCAAC-3'
	Reverse	5'-ACTCAGGCTGGGCATCTGTT-3'
	Probe	5'-AGCCAGAGGATCACCCCGGG-3'
IL6	Forward	5'-GACTTCCATCCAGTTGCCTTCT-3'
	Reverse	5'-CTGTTGGGAGTGGTATCCTCTGT-3'
	Probe	5'-TGACAACCACGGCCTTCCCTACTTCA-3'
IL1 β	Forward	5'-GAGCCATCCTCTGTGACTCA-3'
	Reverse	5'-GTTGTTTCATCTCGGAGCCTGTAG-3'
	Probe	5'-AACCTGCTGGTGTGTGACGTTCCCA-3'
IL12 p35	Forward	5'-GTTGCCTGGCTACTAGAGACTTC-3'
	Reverse	5'-GCACAGGGTCATCATCAAAGAC-3'
	Probe	5'-ACAACAAGAGGGAGCTGCCTGCC-3'
IFN- γ	Forward	5'-GCAACAGCAAGGCGAGAAA-3'
	Reverse	5'-GCTGGATTCCGGCAACAG-3'
	Probe	5'-AGGTCAACAACCCACAGGTCCAGCG-3'